CILASCI 6

Belo Horizonte – Brasil. 27 a 29 de julho de 2022

LIVRO DE RESUMOS DO 6° CONGRESSO IBERO-LATINO-AMERICANO EM SEGURANÇA CONTRA INCÊNDIOS

LIBRO DE RESÚMENES DEL 6° CONGRESO IBERO-LATINO-AMERICANO EN SEGURIDAD CONTRA INCENDIO

ABSTRACT BOOK OF THE 6TH IBERIAN-LATIN AMERICAN CONGRESS ON FIRE SAFETY

EDITORES

Aline Lopes Camargo | João Paulo Correia Rodrigues | João Victor Fragoso Dias | Larice Gomes Justino

THE FIRE RESISTANCE OF LIGHT TIMBER FRAME WALLS WITH DIFFERENT LOAD LEVELS AND CLADDING LAYERS

Paulo A.G. Piloto*
Professor
IPB
Portugal

Diego Vergara
Professor
UCAVILA
Spain

Keywords: Light Timber Frame walls; Fire Resistance; Load level; Charring Rate; Cladding.

1. INTRODUCTION

Lightweight Timber frame walls (LTFW) are commonly used in residential buildings due to their light weight and low construction costs. LTFW are made with solid wood members (studs and tracks) used on buildings, for load-bearing and partition walls. The assemblies are made with solid stud wood vertical members, usually separated by 400 to 600 mm. The cladding for internal walls may be developed by wood panels, composite panels and or gypsum panels. The number of protection layers and insulation materials used in the cavity of the wall depends on the thermal and acoustic efficiency required to the LTFW at room temperature, but also depends on the required fire rating of LTFW.

During the last years, some experimental tests have been carried out. In 1994, Mehaffey et al. [1] developed some experimental tests to validate the 2D numerical model. The model was able to predict the heat transfer with good agreement, even using material properties from the literature. Later in 1998, Takeda and Mehaffey [2] used the same experimental tests to improve the 2D model, improving the description of heat transfer through the entire assembly, in particular across the cavity region. These experimental tests were already used for the validation of the 2D numerical model using Ansys [3], by Piloto and Fonseca. In 2001, Clancy [4] reviewed the progress made in modelling heat transfer through LTF structures exposed to fire, presenting also

* Corresponding author – Departament of Applied Mechanics, Polytechnic Institute of Bragança. Campus Santa Apolonia. 5300-253 Bragança. PORTUGAL. Telef.: +351 273 303157. e-mail: ppiloto@ipb.pt

some experimental results. The model included the implicit motion of moisture and vapour, the modelling of re-entrant corners in void cavities, and the ablation of the gypsum layers. In the same year, Young and Clancy [5] developed a structural model to determine the behaviour of LTFW based on a single stud under fire, following the performance-based building regulations. According to these authors, this closed-form model is accurate, with prediction results within 2% when compared to the numerical results and with good agreement with experimental results. Gypsum boards are also contributing to the initial structural fire resistance of the LTFW, when working in tension and when exposed to low temperatures (below 100 ºC). Different reduction coefficients were used to simulate the behavior of the wood. Load deflection is also compared between the experimental results and the closed-form results for the wall specimen. In 2002, Collier and Buchanan [6] developed a numerical model using finite differences, to predict the fire resistance of non-load bearing or load bearing LTFW when exposed to realistic and standard fire. The model considers the 1D thermal equilibrium to determine the insulation capacity of the LTFW and a special algorithm to determine the non-charred area in order to find the structural stability of the LTFW studs. For the heat transfer across the void cavity, both radiation and convection mode of heat transfer were used, which are in line with the current investigation. The charring rate of this model was determined by the amount of the radiation heat flux. According to these authors, studs in the LTFW are modelled as axially loaded columns and the fire effect is predicted by the residual cross-section in the studs and a calculation of the residual load bearing capacity. Their model does not consider the effect of the timber frame and the effect of other efforts developed during fire. Predicted temperatures were compared with experimental measurements and some differences are noted, although prediction model temperatures are following the tendency of the evolution for standard fire testing. The structural failure was also compared for all the three specimens with a relative performance between 88 and 104.8%. In 2002, Clancy [7] developed a parametric analysis to predict the structural time-to-failure of gypsum cladding LTFW under fire. The study found that the most dominant variables, by order of importance are the depth and the width of studs, the fire scenario, the thickness of the gypsum layer, the elastic modulus of wood in compression, the enthalpy of gypsum and the load applied. These authors concluded that load is not as dominant as could be expected, because doubling the load only affected the time-to-failure by 15%, when using loads within the typical service range, usually less than 25% of the ambient load bearing capacity. They have also concluded that global buckling is the dominant structural failure mode, hence the elastic modulus of wood in compression dominates the strength of wood in determining the time-to-failure, and that the time-to-failure varies inversely with wall height when the load is constant. In 2010, Thomas [8] evaluate the thermal performance analysis for SAFIR and TASEF concerning the temperature results obtained from several experimental tests, analysing the contribution by the gypsum material. This author concluded that both software present good results for slower developing fires and furnace tests when compared with rapidly growing fires. He also concluded about the best thermal properties of gypsum material that should include the effect of two dehydration reactions and a third calcination reaction. Further modification on the thermal properties of gypsum is of limited effect, due to the model limitations regarding the absence of moisture motion, cracking and ablation in gypsum. More recently, Piloto et al. [9] developed a parametric analysis on a 2D model to demonstrate that the fire resistance for insulation depends on the depth and distance between studs, while these parameters are not included in the separating function method presented in the next generation of the EN1995-1-2 [10].

This investigation presents a parametric analysis to find the fire resistance of a LTFW and a new proposal to find this time with respect to the load level, that is only valid for the load level under consideration, changing from 5 to 20%. The load level is defined by the percentage of the load bearing determine at room temperature.

2. STANDARD FIRE TESTING OF LTFW

For the case of load bearing walls, the vertical load is transmitted through the studs and panels may increase the stability of the vertical elements, depending on the stiffness of the connection between the panels and the studs. Panels may be also supporting orthogonal and in plane loads, in the case of external walls submitted to wind loads and seismic loads. The fire resistance should be verified for the load bearing capacity (R), insulation (I) and integrity (E), usually using experimental standard tests, where specimen instrumentation and criteria are defined on EN1363-1 [11], EN1365-1 [12], ISO834 [13]. For the case of non-load bearing walls, the fire resistance should be verified for the insulation (I) and integrity (E), usually using the same type of procedures EN1363-1 [11], EN1364-1 [14], ISO834 [13]. Load bearing and partition wall systems used in residential and commercial properties are required to provide fire rating according to standard EN13501-2 [15], used for the fire classification of construction products and building elements. Partition walls can be rated for EI=15, 20, 30, 45, 60, 90, 120, 180 and 240 (min), while the load bearing elements can be rated for REI=15, 20, 30, 45, 60, 90, 120, 180, 240 and 360 (min). The safety level is then selected by European countries, using their own national level safety system.

The insulation criterion (I) measures the ability of the element to keep the unexposed side with controlled temperatures, tracking the average and maximum temperatures, avoiding the ignition of the materials in the adjacent compartment and fire spread. The criteria define the time, in completed minutes, for which the test specimen continues to maintain its separating function during the test without developing temperatures on its unexposed surface which increase the average temperature above the initial average temperature by more than 140 K, or increase at any location above the initial average temperature by more than 180 K.

The loadbearing criterion (R) measures the ability of the slab to support the imposed load. The criterion is determined from the measurements of the maximum deflection (*C*) or the rate of deflection (*dC/dt*), following the definitions presented in Table 1, where h represents the initial height of the test specimen, once the load is applied.

Table 1: Fire resistance criterion for load bearing (R)

Criterion	Formula	unity
C_{lim}	$h/100$	(mm)
$(dC/dt)_{lim}$	$3h/1000$	(mm/min=

3. MATERIALS, MODELS AND SOLUTION METHODS

This numerical investigation finds the time to structural failure of one timber frame (reduced scale), made with softwood solid timber, protected by one and two gypsum layers. It is assumed that gypsum does not contribute to the load bearing of the timber frame. The LTFW is positioned inside a rigid frame with the bottom end fixed to the frame. The load is applied on top and both lateral edges are free to move down, move out of the plane of the frame and they are restrained to move in-plane towards the frame direction. The external studs are free to move in-plane towards the direction of the central stud.

The elastic buckling analysis was developed to find the critical load and mode of instability. The block Lanczos method [16] has been used to this end. The instability mode has been used to define the geometric imperfection of the timber frame.

The load bearing capacity of the timber frame was determined with an incremental solution and a non-linear geometric and material analysis. This maximum load has been determined using the arc-length method [17].

The thermal analysis considered the effect of the standard fire on the exposed side. Convective and radiative heat flux is considered inside the cavity, based on the bulk cavity temperature of two experimental fire scenarios used for LSF walls developed by Piloto et al. in 2019 [18] and Khetata et al. in 2020 [19]. The model used for single layer protection is exposed to standard fire for 60 minutes and the bulk temperature inside the cavity follows the temperature history “FIRE CAVITY 1”. The model used for double layer protection follows the temperature history “FIRE CAVITY 2” and ran for 120 minutes, see Figure 1.

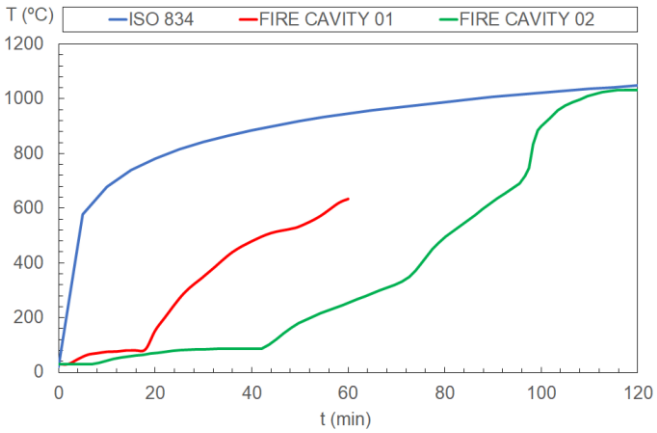

Figure 1: Fire curves used for the simulation of Light Timber Frame Walls

The structural analysis under fire is developed using the Newton Raphson method [20], considering an incremental solution based on a time step of 60 s, with the possibility to be reduced to 0.001 s. The iterative solution is based on a tolerance criterion of 5% in force, using a reference value of 1N.

The LTFW assemblies under evaluation are made with softwood Douglas fir, using 3 solid timber elements for studs and 2 solid timber elements for tracks, each using a cross section of 100 (mm) x 50 (mm). The dimensions are defined according to the expected furnace testing dimensions, see Figure 2.

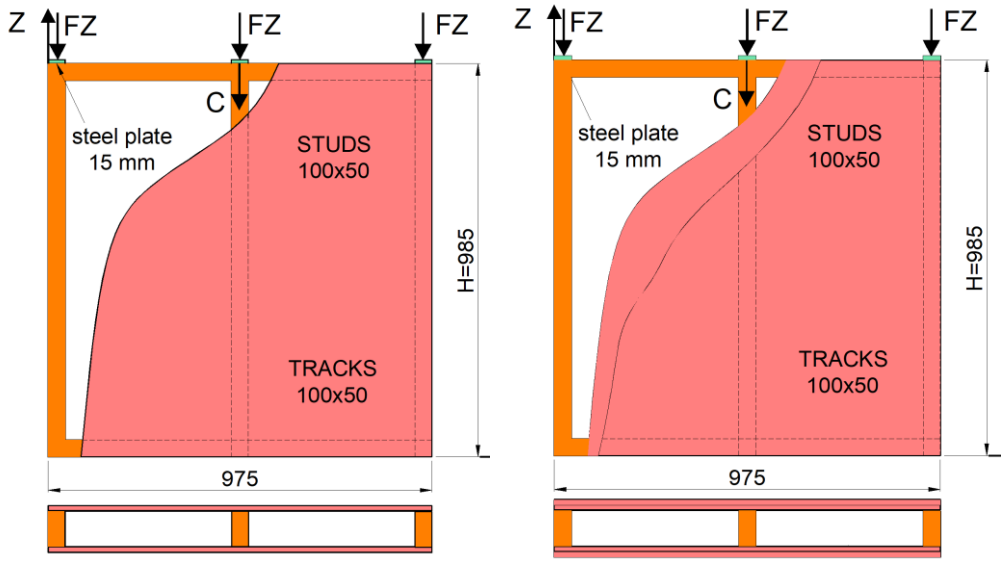

Figure 2: LTFW with one and two gypsum layers

The specimens are simulated according to the conditions presented in Table 2. The fire scenario inside the cavity includes the effect of the cracking, falling off and damage of gypsum plates during experimental tests. This damage effect has been considered by the additional boundary condition inside the cavity, considering the measured cavity temperature as the bulk temperature required for heat transfer by radiation and convection.

Table 2: Identification of specimens

Specimen	Protection layers Gypsum	Fire scenario exposed surface	Fire scenario inside cavity
01	1x12.5 (mm)	ISO 834 [13]	FIRE CAVITY 01 [18] (Specimen 08)
02	2x12.5 (mm)	ISO 834 [13]	FIRE CAVITY 02 [19] (Specimen 11)

The material properties involved in these simulations are the thermal properties for wood and gypsum (conductivity, specific heat density and emissivity) and the mechanical properties for wood members (elastic, plastic, and damage criterion). Gypsum is not considered for load bearing even with the existence of self-screwing bolts.

The thermal properties for both materials involved in simulation are presented in Figure 3 and Figure 4 and they are based on the EN1995-1.2 [21] and based on Sultan investigation [22]. The emissivity used for both materials is 0.8. The thermal behaviour of gypsum considers only two main reactions when exposed to elevated temperatures.

The mechanical properties are only presented for the material that is capable to bear the vertical load. Wood is a highly anisotropic material, due to the way the tree grows and the arrangement of the wood cells within the stem. Wood can be considered locally as an orthotropic material that includes three principal directions. The wood model considers different behaviour of the material in the direction of the fibres, radial direction, and tangential direction. The strength and stiffness of wood are considerably higher in the longitudinal than in the other orthogonal directions. This can be easily understood based on 90 to 95% of the fibres being longitudinally oriented [23]. The generalized Hooke law for an orthotropic material is considered. Table 3 gives the values used for the elastic behaviour of the material.

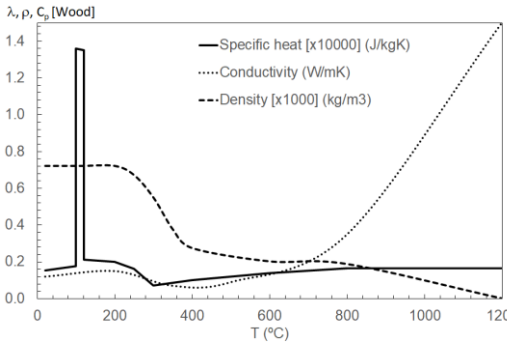

Figure 3: Thermal properties for wood

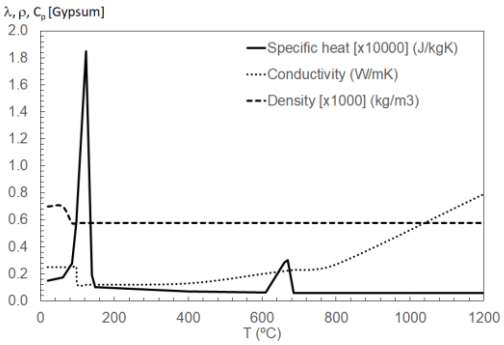

Figure 4: Thermal properties for gypsum

Table 3: Linear elastic orthotropic properties for softwood Douglas fir [21]

	20 (ºC)	100 (ºC)	300 (ºC)
E_X (Pa)	11.20×10^9	5.600×10^9	0.112×10^9
E_Y (Pa)	0.448×10^9	0.224×10^9	0.004×10^9
E_Z (Pa)	0.985×10^9	0.493×10^9	0.009×10^9
ν_{XY}	0.315	0.315	0.315
ν_{YZ}	0.308	0.308	0.308
ν_{XZ}	0.347	0.347	0.347
G_{XY} (Pa)	0.907×10^9	0.454×10^9	0.009×10^9
G_{YZ} (Pa)	0.123×10^9	0.061×10^9	0.001×10^9
G_{XZ} (Pa)	1.075×10^9	0.538×10^9	0.010×10^9

Moreover, According to EN1995-1-2 [15] it is possible to conclude that the strength for wood in the direction parallel to the grain is linearly reduced with increasing temperature, more accentuated up to 100 (°C). The modulus of elasticity is also affected by the increase in temperature, applying the reduction factors between 100 and 300 (ºC). Poisson's coefficients are considered constant in the face of temperature rise, because the current version of the EN1995-1-2 [15] and next generation [10] do not define correction factors to be applied for this property. The transverse elastic modulus also undergoes a reduction with increasing temperature, and the same reduction coefficients of the modulus of elasticity are being used, since both elastic properties of wood are related through Poisson's coefficients. The failure of wood can be presented in several ways, such as fibre breakage, micro-cracking of the matrix, detachment of fibres or delamination. To characterize this effect, the Hill criterion is adopted [24]. This criterion

is based on von Mises's theory and adapted for the application in orthotropic materials. Hill's criterion considers the interaction between the stress in the failure mechanism and depends on the orientation of the stress concerning the orthotropic axis of the material. This criterion allows the determination of the elastic and elastoplastic zones in the stress-strain relationship of the wood. The characteristic parameters of the orthotropic material, defined for this criterion, are the R_{ij} yield rates, which are established as a function of the limit stress in the main directions of the material. knowing that the wood does not have the plastic capacity, the elastic perfectly plastic regime is considered for the constitutive law of this study just to ensure that the material has an elastic limit. The tensile strength f_{xx}^{y} value is 44.49, 28.92 and 0.44 (MPa), for each temperature level (20, 100 and 300 (ºC)) [25]. Table 4 gives the yielding rates used for each orthogonal direction and temperature level.

Table 4: Strength limit in tension and Hill criterion coefficients for softwood Douglas fir [25]

	20 (ºC)	100 (ºC)	300 (ºC)
f^{y} (Pa)	44.90x10^6	28.92x10^6	0.449x10^6
$R_{XX}= f_{xx}^{y}/f^{y}$	1	1	1
$R_{YY}= f_{yy}^{y}/f^{y}$	0.052	0.052	0.052
$R_{ZZ}= f_{zz}^{y}/f^{y}$	0.052	0.052	0.052
$R_{XY}= f_{xy}^{y}/(f^{y}/\sqrt{3})$	0.405	0.405	0.179
$R_{YZ}= f_{yz}^{y}/(f^{y}/\sqrt{3})$	0.405	0.405	0.179
$R_{XZ}= f_{xz}^{y}/(f^{y}/\sqrt{3})$	0.405	0.405	0.179

4. FINITE ELEMENT MODEL FOR THERMAL ANALYSIS

The finite element model considers the hexahedron SOLID70. This element has eight nodes, each with one degree of freedom (temperature), uses linear interpolating functions and full Gauss integration 2x2x2 [26]. The mesh is defined in Figure 5, for both specimens. The number of elements was obtained through a convergence test. The solution method is considered incremental and iterative, due to the non-linearities involved in the materials properties and boundary conditions. The time step was selected to be 60 (s), but can be reduced to 1 (s). The criterion used for convergence of the solution is based on the heat flow, using a tolerance value of 0.1% and a reference value of 10^{-6}. Based on previous numerical research [19], one additional boundary condition is applied to all the internal surfaces of the cavity. The convection coefficient is set to be α_c=17 (W/m²K) and the emissivity of the flames is ε_f=1.0, assuming that the bulk temperature of the cavity is following the fire cavity curves defined in Figure 1. The convection coefficient is an average value between the exposed and unexposed sides [27]. This value may be justified by the fact that the cavity is not directly exposed to fire during all testing time and depends on the gypsum cracking and ablation. The cavity region is not exposed in the beginning, is partially exposed during the test and fully exposed at the end of the test.

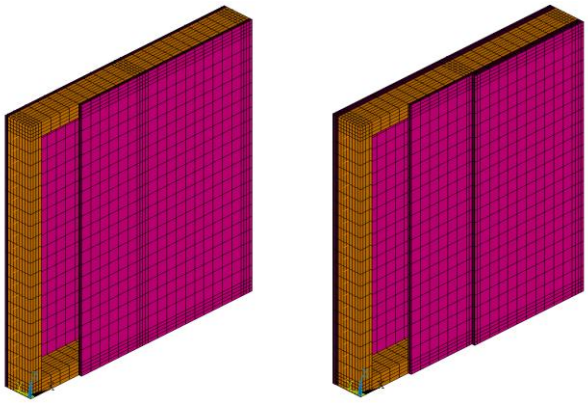

Figure 5: Finite element mesh for both specimens

Results are evaluated for every time step. Figure 6 depicts the temperature field for both materials and the charred zone (identified by the grey colour) of the timber elements, after 30 and 60 (min) of fire exposure.

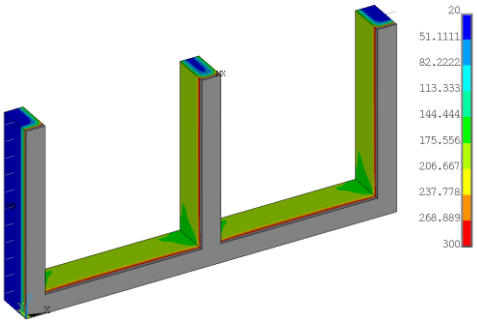

Charred wood after 30 min (specimen 1)

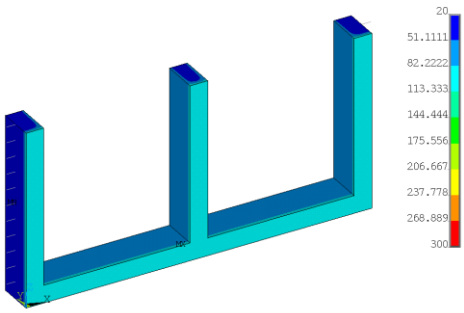

Charred wood after 30 min (specimen 2)

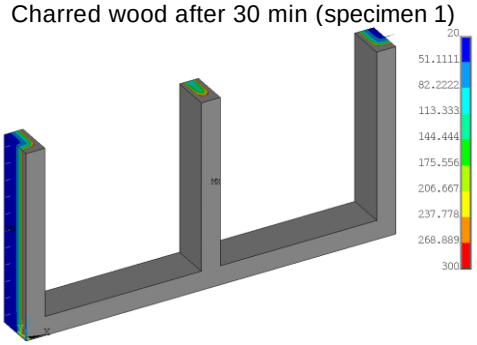

Charred wood after 60 min (specimen 1)

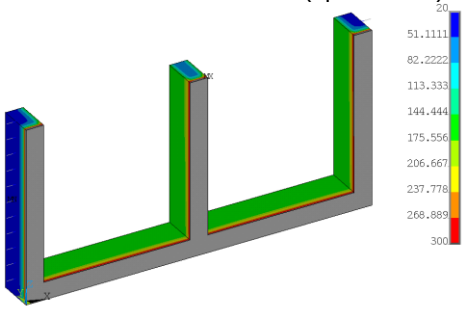

Charred wood after 60 min (specimen 2)

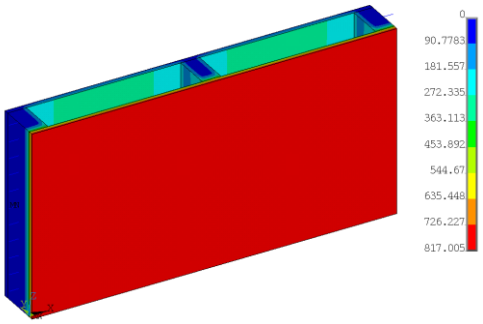

Temperature after 30 min (specimen 1)

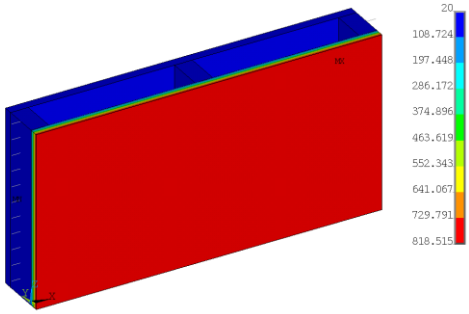

Temperature after 30 min (specimen 2)

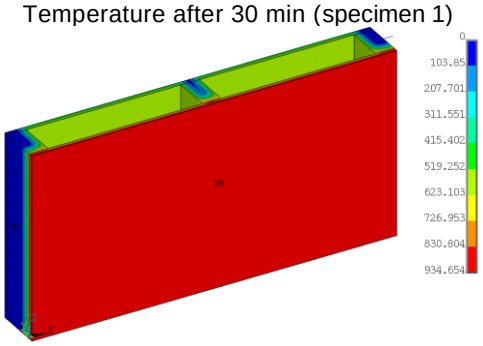

Temperature after 60 min (specimen 1)

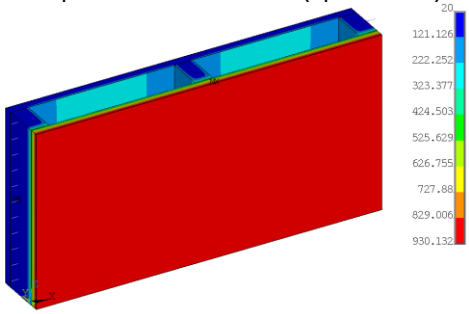

Temperature after 60 min (specimen 2)

Figure 6: Temperature results after 30 and 60 minutes of fire exposure

Specimen 02 has higher fire protection, because it is using a double layer of gypsum plates, which reduces the temperature in both materials for the same time being considered. The charred area of specimen 2 is smaller than specimen 1, especially due to the level of fire protection.

The formation of the char layer may provide effective protection against the heat flux, especially in large cross sections, reducing the charring rate. The failure time of this protection t_f is assumed to be coincident with the time to start the charring formation t_{ch} on the narrow side of the stud. The temperature of the wood surface, at this time, will be submitted to a higher bulk temperature from the fire compartment, conducting to a higher charring rate, until the char layer achieves 25 mm. After that period of time the charring rate decreases, according to the model of EN1995-1-2.

The average and the maximum temperature are also calculated in the unexposed surface to determine the insulation fire resistance. The criterion is based on the increase of the unexposed average temperature (T_{ave}) or the unexposed maximum temperature (T_{max}). Both results are presented in Table 5 and are based on the temperature results of every node located at mid high of the unexposed surface.

Table 5: Fire resistance for insulation (t_{fi})

	T_{max} (min)	T_{ave} (min)
specimen 01	44	46
specimen 02	91	91

5. FINITE ELEMENT MODEL FOR STRUCTURAL ANALYSIS

For the structural analysis, the hexahedron SOLID185 finite element is used. This element has eight nodes, each with three degrees of freedom (translations in each spatial direction UX, UY; UZ), uses linear interpolating functions and full Gauss integration 2x2x2, with enhanced strain calculation [26]. This model also includes an interface element COMBIN39 [26], used to simulate the lateral restrain effect of the simulating frame usually used in the furnace tests. According to the standard EN1365-1 [12], the width of the specimen is less than the opening in the test frame, with a clearance between 25 (mm) to 50 (mm) from the lateral edges of the test specimen. This clearance only restrains the in-plane motion of the wall studs towards the frame, but should not offer any restrain in the opposite direction. This element behaves mainly under a compression load, according to Figure 7.

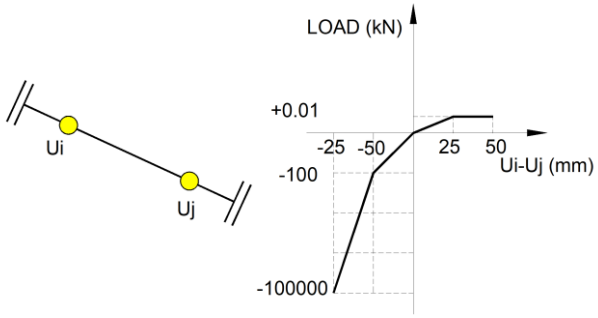

Figure 7: Load-deflection curve for COMBIN39 finite element (not in true scale)

The load bearing is determined for this loading condition, but depends on the initial condition on the geometry and material (imperfections). Different deformed shape modes may be expected for the LTFW structure. A global imperfection, based on the maximum out of straightness equal to H/300 (H = height of the wall), is applied to the first instability mode to update the initial geometry. Using this initial geometry, the vertical load versus the contraction “C” of the structure has been determined at room temperature and for other typical fire rating periods, see Figure 8.

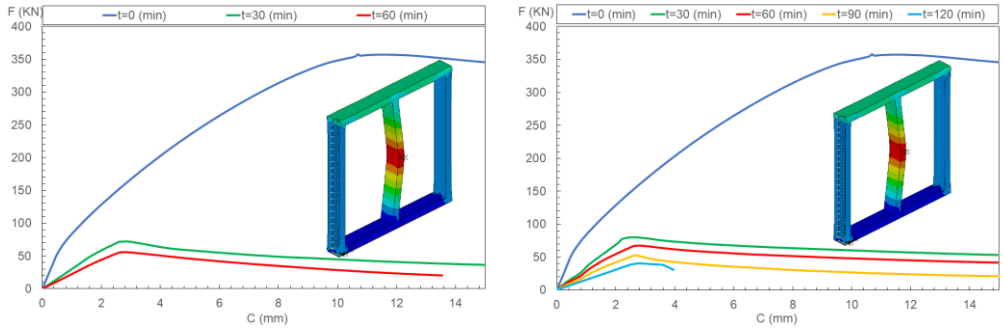

a) Specimen 1 b) Specimen 2

Figure 8: Load bearing capacity of the LTFW at t=0, 30, 60, 90, and 120 min

The solution method is incremental in displacement and iterative. Ansys uses the Newton Raphson method to determine the new equilibrium position for the structure when the displacement on the top is forced to compress the timber frame. The total reaction or load bearing (F) is determined on the top nodes, where the displacement is applied, for each equilibrium position. The incremental displacement is applied on the top of the LTFW structure, with a typical incremental displacement of 0.01 (mm), which can change between 0.001 to 1 (mm), depending on the convergence process. The criterion used to achieve the convergence is based on the internal forces, using a tolerance value of 5%. Here one can assume the existence of the external load {F} must be in equilibrium with the internal forces corresponding to the stress field [σ]. The load bearing relation concerning the vertical contraction has a variable shape. Starts with a linear branch, followed by a non-linear trend up to the maximum load, reached for C=12 (mm). The instability changes the load bearing capacity, being the deformed shape mode of the central stud responsible for the timber frame failure. The maximum load bearing was fixed to 151 (kN), regarding the shape of the load versus displacement of this structure defined for other fire ratings, considering the value for C=2.6 (mm).

This parametric study considers the effect of the load level, changing between 5% and 20% of the maximum load bearing at room temperature. Figure 9 represents the vertical contraction of the timber structure with respect to time. The initial displacement (solid line) is due to the mechanical load, then the LTF reaches a plateau and after a certain period of time the displacement tends to increase very fast, reaching the displacement limit. This is the time when the LTF reaches a very big rate of displacement (dashed line). This figure also represents the rate of displacement and both limits for *C*=10 (mm) and *dC/dt*=3 (mm/min). The LTF is deformed and all simulated models attained the global bucking deformed shape mode, with studs moving to the outside of the furnace, due to the effect of load and charred layer, see Figure 10.

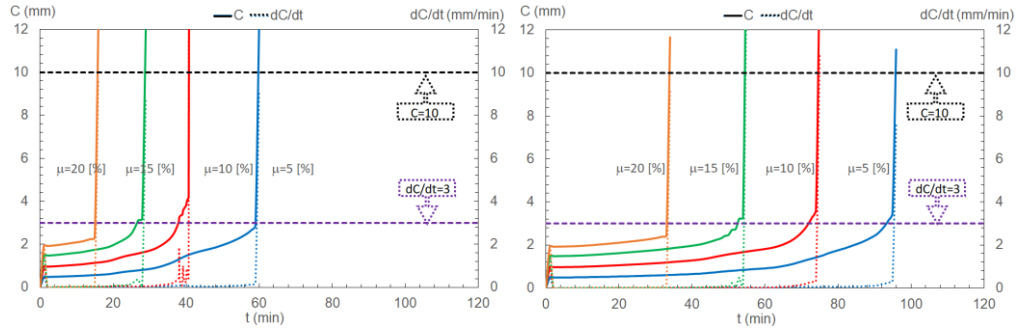

a) specimen 01 (one gypsum layer). b) specimen 02 (two gypsum layer).

Figure 9: Load level effect on the fire resistance

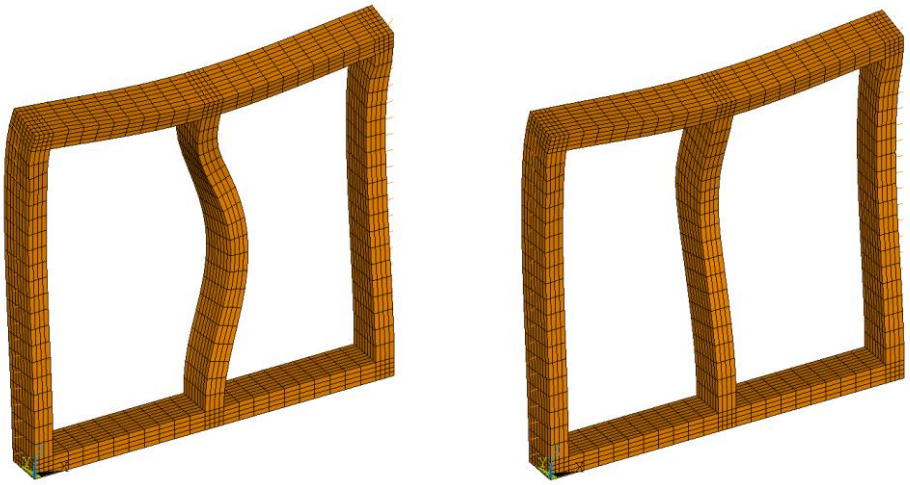

a) Specimen 01 (one gypsum layer). b) Specimen 02 (two gypsum layer).

Figure 10: Deformed shape mode

The fire resistance of a double protected LTFW is higher than the fire resistance of a single protected LTFW, and both decrease with the load level. The fire resistance changes linearly with the load level. A new proposal is presented between the fire resistance t_{fi} and the load level μ, see Equation 1.

specimen 1	$t_{fi}=-293.5\times\mu+72.8$	(1)
specimen 2	$t_{fi}=-409.0\times\mu+115.4$	(2)

6. CONCLUSIONS

The ability to sustain the temperature bellow a certain level in the unexposed side of the LTF wall (insulation criterion- I) is higher when using two gypsum layers. This ability is reduced by 50% when using one single layer of gypsum. The ability to sustain the load of the LTF (load bearing criterion – R) is also higher for the case of the LTF wall protected by two gypsum layers. This ability is reduced by 46%, on average, when using only one gypsum layer. The timber frame is deformed under fire and all simulated models attained the global bucking instability mode, with studs moving to the outside of the furnace, due to the effect of load and charred layer. Some specimens also included flexural buckling with respect to minor axis, for the last time increment of equilibrium. The fire resistance of a double-layered protected LTF wall is higher than a single-layered LTF wall, and both decrease with the load level. The numerical criterion used to stop the simulation, in order to define the ability to sustain the load, is defined by the last stable equilibrium configuration. This configuration has always passed the time defined by the criteria used in the experimental standard EN1361-1, regarding the critical maximum contraction displacement and rate of displacement. A new formula is also proposed to define this ability, based on the fire resistance and the load level.

REFERENCES

[1] J. R. Mehaffey, P. Cuerrier, and G. Carisse, “A model for predicting heat transfer through gypsum-board/wood-stud walls exposed to fire,” *Fire Mater.*, vol. 18, no. 5, pp. 297–305, Sep. 1994, doi: 10.1002/fam.810180505.

[2] H. Takeda and J. R. Mehaffey, “WALL2D: A model for predicting heat transfer through wood-stud walls exposed to fire,” *Fire Mater.*, vol. 22, no. 4, pp. 133–140, Jul. 1998, doi: 10.1002/(SICI)1099-1018(1998070)22:4<133::AID-FAM642>3.0.CO;2-L.

[3] P. A. G. Piloto and E. M. M. Fonseca, “Timber Framed Walls Lined With Gypsum Plates Under Fire,” in *7th International Conference Integrity-Reliability-Failure*, 2020, pp. 547–556.

[4] P. Clancy, “Advances in modelling heat transfer through wood framed walls in fire,” *Fire Mater.*, vol. 25, no. 6, pp. 241–254, 2001, doi: 10.1002/fam.773.

[5] S. A. Young and P. Clancy, “Structural modelling of light-timber framed walls in fire,” *Fire Saf. J.*, vol. 36, no. 3, pp. 241–268, Apr. 2001, doi: 10.1016/S0379-7112(00)00053-9.

[6] P. C. R. Collier and A. H. Buchanan, “Fire resistance of lightweight timber framed walls,” *Fire Technol.*, vol. 38, no. 2, pp. 125–145, 2002, doi: https://doi.org/10.1023/A:1014459216939.

[7] P. Clancy, “A parametric study on the time-to-failure of wood framed walls in fire,” *Fire Technol.*, vol. 38, no. 3, pp. 243–269, 2002, doi: 10.1023/A:1019882131985.

[8] T. Gernay, “Modelling thermal performance of gypsum plasterboard-lined light timber frame walls using SAFIR and TASEF,” *Fire Mater.*, vol. 34, no. 8, pp. 385–406, Dec. 2010, doi: 10.1002/fam.1026.

[9] P. A. G. Piloto, S. Rodríguez-del-Río, and D. Vergara, “Fire Analysis of Timber-Framed Walls Lined with Gypsum,” *Materials (Basel).*, vol. 15, no. 3, p. 741, Jan. 2022, doi: 10.3390/ma15030741.

[10] CEN, “pr EN 1995-1.2, Eurocode 5: Design of timber structures - Part 1-2: General - Structural fire design.” CEN - European Committee for Standardization, Brussels, 2020.

[11] CEN, “EN 1363-1: Fire resistance tests Part 1 : General Requirements.” CEN- European Committee for Standardization, Brussels, p. 52, 2020.

[12] CEN, *EN 1365-1: Fire resistance tests for loadbearing elements - Part 1: Walls*, CEN. Brussels: CEN, 2013.

[13] ISO, *ISO834-1: Fire-resistance tests - Elements of building construction - Part 1: General requirements*. International Organization for Standardization, 1999.

[14] CEN, *EN 1364-1: Fire resistance tests for non-loadbearing elements. Part 1: Walls*, CEN. Brussels: CEN, 2015.

[15] CEN, *EN 13501-2: Fire classification of construction products and building elements - Part 2: Classification using data from fire resistance tests, excluding ventilation services*, CEN. Brussels: CEN, 2016.

[16] C. Rajakumar and C. R. Rogers, “The Lanczos algorithm applied to unsymmetric generalized eigenvalue problem,” Int. J. Numer. Methods Eng., vol. 32, no. 5, pp. 1009–1026, Oct. 1991, doi: 10.1002/nme.1620320506.

[17] E. Riks, “An Incremental Approach To the Solution,” Int. J. Solids Struct., vol. 15, no. 7, pp. 529–551, 1979, doi: https://doi.org/10.1016/0020-7683(79)90081-7.

[18] Paulo Piloto, M. Khetata, and A. Gavilán, “Fire Resistance Tests of Non-Loadbearing LSF Walls,” in *TEST&E 2019 - 2nd Conference on Testing and Experimentations in Civil*

Engineering - Proceedings, 2019, pp. 429–440, doi: http://doi.org/10.5281/zenodo.3355354.
[19] S. M. Khetata, P. A. G. Piloto, and A. B. R. Gavilán, “Fire resistance of composite non-load bearing light steel framing walls,” *J. Fire Sci.*, vol. 38, no. 2, pp. 136–155, Mar. 2020, doi: 10.1177/0734904119900931.
[20] K. -J Bathe, E. Ramm, and E. L. Wilson, “Finite element formulations for large deformation dynamic analysis,” Int. J. Numer. Methods Eng., vol. 9, no. 2, pp. 353–386, 1975, doi: 10.1002/nme.1620090207.
[21] CEN, “EN 1995-1.2, Eurocode 5: Design of timber structures - Part 1-2: General - Structural fire design.” CEN - European Committee for Standardization, Brussels, pp. 1–69, 2004.
[22] M. A. Sultan, “A model for predicting heat transfer through noninsulated unloaded steel-stud gypsum board wall assemblies exposed to fire,” *Fire Technol.*, vol. 32, no. 3, pp. 239–259, 1996, doi: 10.1007/BF01040217.
[23] S. Holmberg, K. Persson, and H. Petersson, “Nonlinear mechanical behaviour and analysis of wood and fibre materials,” *Comput. Struct.*, vol. 72, no. 4, pp. 459–480, 1999, doi: 10.1016/S0045-7949(98)00331-9.
[24] H. Rodney and R. Soc, “A theory of the yielding and plastic flow of anisotropic metals,” Proc. R. Soc. London. Ser. A. Math. Phys. Sci., vol. 193, no. 1033, pp. 281–297, May 1948, doi: 10.1098/rspa.1948.0045.
[25] T. H. Milhan, “Numerical study on wooden beams subjected to high temperatures (in Portuguese),” Instituto Politécnico de Bragança (MSc thesis), 2020.
[26] ANSYS INC., “ANSYS® Academic Research, Release 2021 R2, Help System, Element reference, ANSYS, Inc.” 2021.
[27] CEN, “EN 1991-1-2, Eurocode 1: Actions on structures – Part 1-2: General actions – Actions on structures exposed to fire,” CEN- European Committee for Standardization. CEN-European Committee for Standardization, Brussels, p. 59, 2002.